Dynamic Power and Bit Allocation Scheme for Spectral Efficiency Maximization in Cognitive Multiband OFDM UWB Systems

Liaoyuan Zeng
Wireless Access Research Center
University of Limerick
Limerick, Ireland
Email: liaoyuan.zeng@ul.ie

Sean McGrath
Wireless Access Research Center
University of Limerick
Limerick, Ireland
Email: sean.mcgrath@ul.ie

Eduardo Cano
Institute for the Protection and
Security of the Citizen
Joint Research Center
European Commission
Ispra, Italy
Email: eduardo.cano@jrc.ec.europa.eu

***Abstract*—A novel dynamic power and bit allocation scheme for spectral efficiency maximization in the Cognitive Ultra Wideband radio system is presented in this paper. A new bit error rate expression is derived based on approximating a sum of independent log-normal random variables as a single log-normal random variable using the Fenton-Wilkinson method in order to analyze the spectral efficiency in the UWB multipath channel. A series of M-ary quadrature amplitude modulation zones can be generated over each UWB subcarrier by manipulating the BER expression. The total transmitted power is optimally distributed among the UWB subcarriers for the use of those zones with a maximum M on each subcarrier. The power and bit allocation is divided into primary allocation and advanced allocation for efficient implementation. The performance of the dynamic allocation algorithm is analyzed over different UWB fading channels. The results show that the spectral efficiency of the system is significantly improved by an optimal power and bit allocation techniques.**

***Keywords*-Ultra Wideband; Multiband Orthogonal Frequency Division Multiplexing; Bit Error Rate; Cognitive Radio.**

I. INTRODUCTION

Radio spectrum is a scarce resource, both dynamic power allocation and adaptive spectrum sharing through cognitive radios can significantly enhance the spectrum utilization in a wireless network [1][2]. The principle behind cognitive radio consists of defining and developing technologies that can enable a radio device to sense the states of the frequency bands and adapt its internal states to statistical variations in the incoming RF stimuli by making corresponding changes in certain operation parameters in real-time. Thus, a cognitive (unlicensed/secondary) system can detect and access the temporarily-unused spectrum very rapidly without interfering with the primary (licensed) systems (e.g., WiMAX).

Several physical-layer radio platforms have been suggested for cognitive radio networks, one of the leading candidates is Multiband Orthogonal Frequency Division Multiplexing (MB-OFDM) Ultra Wideband (UWB) system [3][4]. UWB systems use signals with a fractional bandwidth greater than 0.20 or occupy a minimum of 500 MHz (-10 dB) bandwidth in the 3.1–10.6 GHz frequency band with a maximum mean Power Spectral Density (PSD) of -41.3dBm/MHz [5]. The UWB bandwidth is subdivided into a number of orthogonal subcarriers (subchannels) with bandwidth of each less than the channel coherence bandwidth. Hence, the Intersymbol Interference (ISI) caused by multipath fading is minimized when the information is transmitted over different subcarriers. Furthermore, the MB-OFDM scheme can significantly enhance the flexibility and ease of dynamically allocating unused spectrum in cognitive UWB radio systems [4].

A novel dynamic power and bit allocation scheme for spectral efficiency maximization in the cognitive MB-OFDM UWB radio systems in a multipath fading channel is presented in this paper. This work in based on our previous work [1] which did not integrate the cognitive radio technology into the UWB systems. Furthermore, for an in-depth spectral efficiency analysis of UWB multipath channel, a new Bit Error Rate (BER) expression is derived based on approximating a sum of independent log-normal random variables as another log-normal random variable using the Fenton-Wilkinson method [6]. The optimization of the spectral efficiency is under the constraints in probability of detection and false alarm, transmission PSD and BER. The objective is to maximize the number of the information bits loaded in the UWB subcarriers (each with different levels of fading [7]) by optimally allocating the available total transmitted power while guaranteeing a sufficient protection to the primary users.

By exploiting the channel conditions, a cognitive UWB system can opportunistically access the temporarily-unused spectrums and implement the optimal power and bit allocation schemes. The fraction of time for UWB data transmission is constrained by the spectrum sensing period and the probability that the primary user is transmitting or receiving within the spectrum of the UWB subcarriers. It is assumed that this probability follows a Poisson process. The information bits assigned in each subcarrier are modulated using M-ary Quadrature Amplitude Modulation (M-QAM) modulation. Thus, it is required to use the modulation scheme with the

maximum M in the subcarrier to maximize the spectral efficiency.

The paper is organized as follows. In Section II, a literature review of the spectral efficiency optimization in cognitive multicarrier systems is presented. Next, the system model is discussed in Section III, including the discussion of the UWB multipath propagation, the multiband OFDM scheme and the cognitive UWB radio systems. In Section IV, a new in-depth BER performance analysis is carried out. On the basis of the BER analysis, the system spectral efficiency is analyzed in Section V. Then, the design of the dynamic power and bit allocation algorithm is provided in Section VI. The analysis of the simulation results is carried out in Section VII. Finally, conclusions are presented in Section VIII.

II. Literature Review

The discussion of the UWB cognitive radio systems optimization with respect to spectrum sensing and dynamic spectrum sharing has been treated extensively in the literature dedicated to wireless systems and theory [3][8][9][10]. As an optimization problem in multicarrier transmission systems, the spectral efficiency maximization problem (in terms of how to optimally allocate bits and power to UWB subcarriers) is originally a non-convex integer-programming optimization problem which is generally NP-hard [9]. The common solution is either to relax this non-convex optimization problem into a convex optimization problem or to use some metaheuristic algorithm such as greedy algorithm to approximate the optimal solution [9][11].

The theoretical capacities achieved by the cognitive Impulse Radio (IR) UWB systems with constraints in outage probability of the primary users were studied in [3]. The authors in [4] proposed a power allocation scheme using Lagrange formulation to maximize the total transmission capacity of the OFDM-based cognitive users. In [12], the effects of the multipath fading channel on the choice of the transmitted power level were taken into account for the design of the cognitive power control strategies for system ergodic capacity maximization. These addressed the fundamental channel rate limits of the cognitive radio systems from a information theory perspective.

Furthermore, in the derivation of the MB-OFDM UWB BER expression in [13][14], the authors assumed that the multipath gain coefficients of the UWB channel model have a statistically independent Gaussian distribution with zero mean and variances. Authors in [15] made similar assumptions and approximated the UWB channel frequency response to a Rayleigh fading channel. In this paper, a more accurate BER expression is derived based on the log-normal distribution of the UWB multipath gain coefficient. The UWB channel measurement studies [5][16][17][18][19] have suggested that the log-normal distribution can more accurately reflect the measurement data.

III. System Model

This section provides a review of the MB-OFDM UWB systems and cognitive UWB radio systems, and specifically focuses on the introduction of the MB-OFDM schemes.

A. UWB Signal

The MB-OFDM UWB transmitted signal of the node u is represented by

$$x^{(u)}(t) = \sum_{i=-\infty}^{+\infty} \frac{1}{T_S} \sum_{n=0}^{N_{FFT}-1} c_{n,i} g(t - iT_S^{'}) e^{\frac{j2\pi n(t-iT_S^{'})}{T_S}}, \quad (1)$$

where T_S is the duration of the useful OFDM symbol and N_{FFT} is the number of subcarriers and also the number of points of the Inverse Discrete Fourier Transform (IDFT). The total duration of the OFDM symbol is computed as $T_S^{'} = T_S + T_{cp} + T_G$ where T_{cp} is the duration of the cyclic prefix for ISI mitigation and T_G is the duration of the guard interval that ensures a smooth transition between two consecutive OFDM symbols. The data sequence in (1) is expressed as $\mathbf{c} = c_{0,i}, c_{1,i}, .., c_{n,i}, .., c_{N-1,i}$ being i the OFDM symbol index and n the subcarrier index. Finally, the function $g(t)$ represents the unitary rectangular pulse of duration T_S. In this work, it is assumed that each data symbol is normalized to have unit energy.

B. UWB Channel

In this work, the UWB multipath channel is modeled by using the Saleh-Valenzuela (S-V) model which captured the clustering phenomenon through practical channel measurements [5]. This UWB channel model is assumed to be linear time-invariant during the transmission of a data packet. The impulse response of the UWB multipath channel with J multipath components is expressed as

$$\mathbf{h}(t) = \sum_{j=0}^{J} \alpha_j \delta(t - T_j), \quad (2)$$

where α_j are the multipath gain coefficients which denotes the amplitude of multipath components subjected to log-normal distribution [16].

The multipath gain coefficients α_j are given by:

$$\alpha_j = p_j \xi_j, \quad (3)$$

where p_j is equiprobable ± 1 to account for signal inversion due to reflections, ξ_j reflects the log-normal fading associated with the jth multipath component. This log-normal variable can be expressed in terms of Gaussian random variable as:

$$\xi_j = 10^{\frac{x_j}{20}}, \quad (4)$$

where x_j is a normal random variable with mean μ_j and variance σ^2. The μ_j is given by:

$$\mu_j = \frac{10ln(\Omega_0) - 10\frac{T_j}{\Gamma}}{ln(10)} - \frac{(\sigma^2)ln(10)}{20}, \quad (5)$$

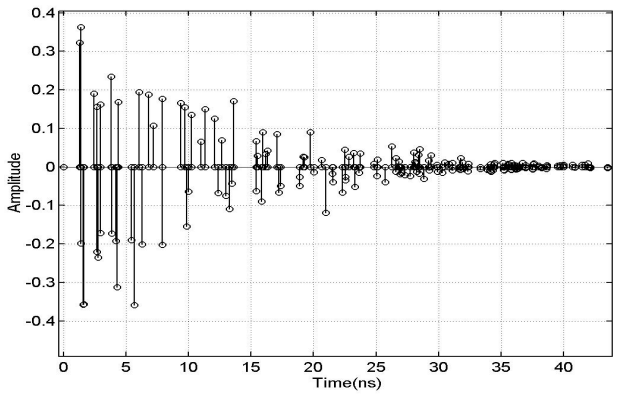

Fig. 1. Impulse Response over CM3

where Ω_0 is the mean energy of the first arrived multipath component, and Γ is the signal decay factor.

The order of $L = J$ is determined by $L = T_d/T_s$, where T_d is the maximum delay spread of the UWB channel, and T_s is the M-QAM symbol period. Hence, it is assumed that the delay between the multipath components is $T = \tau = T_s$ for the reasons of both analytical convenience and sampling processing at the receiver [20]. This assumption is well suited to dense scattering environments. The discrete time version of $\mathbf{h}(t)$ can be expressed as $\mathbf{h} = \mathbf{h}(t)|_{t=lT_s} = \{h(0), h(1), ..., h(L-1)\}$, where $h(l)$ $(l \in [0, L-1])$ is the impulse response of the lth path.

There are four types of UWB Channel Models (CMs) defined based on the practical measurements of the key channel parameters such as mean excess delay and Root Mean Square (RMS) delay spread [5]. A channel impulse response realization for CM3 is represented in Figure 1.

C. Multiband-OFDM Scheme

In MB-OFDM scheme [5], the 3.1–10.6 GHz UWB bandwidth is divided into fourteen sub-bands, each with 528 MHz. An OFDM symbol is transmitted within one sub-band. In each sub-band, a total number of 128 orthogonal subcarriers are used for data transmission.

In a UWB transmitter, the outgoing data packet is first encoded using punctured convolutional code. Then, the coded data is interleaved and modulated into a series of complex M-QAM symbols $\mathbf{S}_n = [S_n(0), S_n(1), ..., S_n(N-1)]^T$ of length $N = 128$, where column vector $\mathbf{S}_n$ represents the nth transmitted OFDM symbol, and $S_n(i)$ $(i \in [0, N-1])$ stands for a single M-QAM symbol. Note that the system performance is not addressed with the Forward Error Correction (FEC) coding in this paper. It is assumed that the data packet transmitted is not encoded. The discrete N-point Inverse Fast Fourier Transform (IFFT) is employed to perform the subcarrier modulation. Thus, the frequency domain signal $\mathbf{S}_n$ is transformed into a real-valued time domain signal $\mathbf{s}_n = \mathbf{F}\mathbf{S}_n = [s_n(0), s_n(1), ..., s_n(N-1)]^T$, where $\mathbf{F}$ is a square IFFT matrix with (i,k)th entry as $\mathbf{F}(i,k) = \frac{1}{\sqrt{N}} e^{j2\pi ik/N}$ $(i,k \in [0, N-1])$. Since the subcarriers are orthogonal to each other, there will be no Inter-Carrier-Interference (ICI) between the $\mathbf{s}_i$ modulated subcarriers. Note that the transmission channel modeled as a linear time invariant channel during the transmission of a data packet.

The ith received time domain sequence $\mathbf{r}_i = [r_i(0), r_i(1), ..., r_i(N-1)]^T$ is the result of the linear convolution between $\mathbf{h}(l)$ and $\mathbf{s}_i = [s_i(0), s_i(1), ..., s_i(N-1)]^T$

$$r_i(n) = \sum_{l=0}^{L-1} s_i(l)h(n-l) + \eta(n). \quad (6)$$

Thus, the ith received frame $\mathbf{r}_i$ can be expressed as

$$\mathbf{r}_i = \mathbf{h}\mathbf{s}_i + \eta_i, \quad (7)$$

where $\mathbf{h}$ is a $N \times N$ Toeplitz matrix which can transfer the above convolution operation into a matrix multiplication [7], i.e.

$$\mathbf{h} = \begin{pmatrix} h(0) & 0 & 0 & \dots & 0 \\ h(1) & h(0) & 0 & \dots & 0 \\ \vdots & \vdots & \vdots & \vdots & \vdots \\ h(L-1) & h(L-2) & \dots & \dots & 0 \\ \vdots & \vdots & \vdots & \vdots & \vdots \\ 0 & 0 & h(L-1) & \dots & h(0) \end{pmatrix}. \quad (8)$$

However, if the ith frame $\mathbf{s}_i$ is transmitted immediately after the $i-1$th frame $\mathbf{s}_{i-1}$, the first $L-1$ symbols of $\mathbf{s}_i$ will be corrupted by the delayed version of the last L symbols of $\mathbf{s}_{i-1}$. When the $(N-L+1)$th symbol $s_{i-1}(N-L+1)$ of $\mathbf{s}_{i-1}$ is transmitted at time $(N-L+1)T_s$, the delayed component of $s_{i-1}(N-L+1)$ will last $(L-1)T_s$ and corrupt with the first symbol of $\mathbf{s}_i$ at time LT_s. Thus, the delayed component of the last symbol $s_{i-1}(N-1)$ transmitted at time $(N-1)T_s$ will corrupt with the first $(L-1)$th symbol of $\mathbf{s}_i$. This type of corruption is so-called Inter-Frame-Interference (IFI) or Inter-Block-Interference (IBI).

Hence, the received frame is expressed as

$$\mathbf{r}_i = \mathbf{h}\mathbf{s}_i + \mathbf{h_d}\mathbf{s}_{i-1} + \eta_i, \quad (9)$$

where $\mathbf{h_d}$ is also a $N \times N$ Toeplitz matrix

$$\mathbf{h_d} = \begin{pmatrix} 0 & \dots & h(L-1) & \dots & h(1) \\ 0 & \dots & 0 & \dots & 0 \\ \vdots & \vdots & \vdots & \vdots & \vdots \\ 0 & \dots & 0 & \dots & h(L-1) \\ \vdots & \vdots & \vdots & \vdots & \vdots \\ 0 & \dots & 0 & \dots & 0 \end{pmatrix}. \quad (10)$$

To eliminate the corruption between received frames, the time domain sequence $\mathbf{s}_n$ is tail attached by a zero-padded suffix (ZPS) of length L [5]. More importantly, appending the ZPS can manipulate the linear convolution between $\mathbf{s}_n$ and the UWB channel impulse response $\mathbf{h}(t)$ into a circular convolution by implementing the time-domain aliasing

[21]. Thus, the ith received frequency domain signal, $\mathbf{R}_n = [R_n(0), R_n(1), ..., R_n(N-1)]^T$, can be expressed as

$$\mathbf{R}_n = \mathbf{F}^{-1}\tilde{\mathbf{H}}\mathbf{F}\mathbf{S}_n + \eta_n, \tag{11}$$

where η_n is the noise figure, and $\tilde{\mathbf{H}} = \mathbf{RhZ}$ is a $N \times N$ circulant matrix with its (i,l)th entry given by $h((i-l)\ mod\ N)$, where $\mathbf{R}$ and $\mathbf{Z}$ are the ZPS attaching and removing matrix [7]. The expression $\mathbf{F}^{-1}\tilde{\mathbf{H}}\mathbf{F} = \mathbf{H} = \text{diag}[H(0), H(1), ..., H(N-1)]$ is a $N \times N$ diagonal matrix. By taking the fourier transform of $h(t)$, the transfer function of the ith MB-OFDM UWB subcarrier $H(i)$ $(i \in [0, N-1])$ can be obtained. $H(i)$ is specified as

$$H(i) = H(2\pi i/N) = \sum_{l=0}^{L-1} h(l)e^{-j2\pi il/N}, \tag{12}$$

It is assumed that $H(i)$ is known at the receiver. Figure 2 shows an example of channel frequency response for CM3.

D. Cognitive MB-OFDM UWB Systems

In this paper, it is considered that the cognitive UWB systems can only access the spectrum of the subcarrier when the spectrum is not occupied by any primary user. Thus, the spectrum sensing process determines the probability that a subcarrier is utilized by the cognitive UWB system. The key parameters for evaluating the performance of sensing are the probability of a false alarm P_f and the probability of detection P_d [22]. An energy detection method is adopted in this work, since energy detection does not need any information of the signal to be detected and is robust to unknown dispersed channel and fading [23].

The amount of time needed for a successful spectrum sensing is denoted as a sensing period τ_s. The fraction of time for data transmission is limited by the value of τ_s as $\alpha = \frac{T_{txop} - \tau_s}{T_{txop}}$, where T_{txop} is a pre-defined transmission period in the UWB MAC layer for different Access Categories (ACs) [24], called Transmission Opportunity (TXOP). An application with $T_{txop} = 512$ μs (ACs) is chosen in this work to be activated in the cognitive UWB system.

For an energy detector, the required sensing period τ_{s_i} according to the target probability of false alarm $\tilde{P_f}$ and probability of detection $\tilde{P_d}$ can be determined as

$$\tau_{s_i} = \frac{2}{\gamma_p^2 f_s}(Q^{-1}(\tilde{P_f}) - Q^{-1}(\tilde{P_d}))^2, \tag{13}$$

where $Q(z) = \int_z^\infty \frac{1}{\sqrt{2\pi}} e^{-y^2/2} dy$ is the complementary distribution function of the standard Gaussian, γ_p is the received Signal-To-Noise Ratio (SNR) of the primary user signals (SNR_p) at the cognitive UWB user, and f_s is the UWB receiver sampling frequency [23].

IV. BER Performance Analysis

The averaged probability of error of MB-OFDM UWB system is computed by integrating the error probability in Additive White Gaussian Noise (AWGN) channel over the UWB fading distribution. In (11), it is demonstrated that the amplitude variations in the received signal are due to the characteristics of the UWB multipath channel. Since α_j in (2) is modeled as a series of independent (uncorrelated) log-normal random process, the distribution of the $|H(i)|$ at the ith subcarrier can be derived from the manipulating the sum of independent log-normal variables α_j. Although an exact closed-form expression for the probability density function (PDF) of a sum of independent log-normal random variables does not exist, the superposition of log-normal variables can be well approximated by a new log-normal distribution using Fenton-Wilkinson method [6].

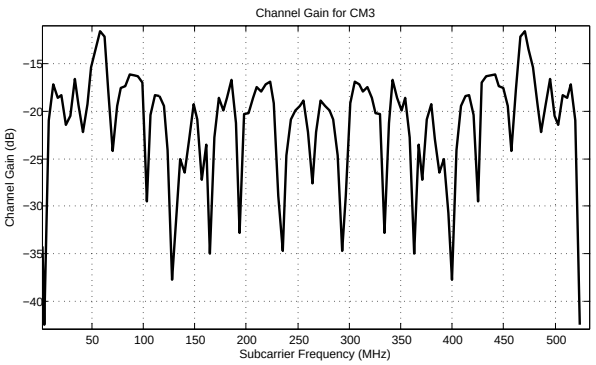

Fig. 2. Frequency response over CM3

It is illustrated in (4) that the jth random variable x has the Gaussian distribution

$$p_X(x) = \frac{1}{\sqrt{2\pi}\sigma_x} e^{-\frac{(x-\mu_x)^2}{2\sigma_x^2}}, \tag{14}$$

where $[\mu_x, \sigma_x]$ are the mean and standard deviation of x. Then, the probability distribution of $\xi_j = 10^{x_j/20}$ can be expressed as a log-normal distribution:

$$p_\xi(\varepsilon) = \frac{20/ln10}{\varepsilon\sigma_x\sqrt{2\pi}} e^{-\frac{(20log_{10}\varepsilon - \mu_x)^2}{2\sigma_x^2}}. \tag{15}$$

The received signal amplitude $|H(i)| = r$ on the ith subcarrier has the distribution of the sum of log-normal random variables α_j. There is a general consensus that the sum of independent log-normal random variables can be approximated by another log-normal random variable with appropriately chosen parameters [25][26]. Therefore,

$$p(r) = \sum_{j=1}^{J} 10^{\xi_j/20} = 10^{Z/20} = p\hat{(r)}, \tag{16}$$

where Z is a Gaussian random variable with mean μ_z and variance σ_z^2.

In Fenton-Wilkinson method, the value of μ_z and σ_z^2 can be calculated by

$$\mu_z = \xi^{-1}(\frac{\sigma_{\hat{\xi}}^2 - \sigma_{\hat{z}}^2}{2} + ln(\sum_{j=1}^{J} e^{\hat{\mu_j}})), \tag{17}$$

$$\sigma_z^2 = \xi^{-2}(ln((e^{\sigma_{\hat{\xi}}^2} - 1)\frac{\sum_{j=1}^{J} e^{2\hat{\mu_j}}}{(\sum_{j=1}^{J} e^{\hat{\mu_j}})^2} + 1)), \tag{18}$$

where $\xi = ln10/20$, $\sigma_{\hat{\xi}}^2 = \xi^2\sigma^2$, and $\hat{\mu_j} = \xi\mu_j$.

Therefore, the distribution of the received signal amplitude r can be expressed as

$$p(r) = \frac{20/ln10}{r\sigma_z\sqrt{2\pi}} e^{-\frac{(20log(r)-\mu_z)^2}{2\sigma_z^2}}. \quad (19)$$

From (19), the distribution of the received SNR per symbol $p_{\gamma_s}(\gamma)$ can be expressed as

$$p_{\gamma_s}(\gamma) = \frac{10/ln10}{\gamma\sigma_z\sqrt{2\pi}} e^{-\frac{(10log(\gamma N_0/E_s)-\mu_z)^2}{2\sigma_z^2}}. \quad (20)$$

For more convenient calculation of $p_{\gamma_s}(\gamma)$, the parameter N_0/E_s can be replaced with $E(r^2)\gamma/\bar{\gamma_s}$ in the equation above since the average SNR per symbol $\bar{\gamma_s} = E(r^2)\frac{E_s}{N_0}$, where $E(r^2)$ is the mean value of the signal power distribution. The expression of $E(r^2)$ can be easily derived by manipulating (19) and expressed as

$$E(r^2) = E(R) = e^{\frac{\mu_z}{10/ln10} + \frac{\sigma_z^2}{2*(10/ln10)^2}}. \quad (21)$$

The averaged probability of symbol error and bit error in UWB multipath fading channel can be computed by averaging the error probability in AWGN $P_s(\gamma)$ over the UWB fading distribution $p_{\gamma_s}(\gamma)$ [27]:

$$\bar{P_s} = \int_0^\infty P_s(\gamma)p_{\gamma_s}(\gamma)d\gamma. \quad (22)$$

In arriving at the error rate results in equations, it is assumed that timing and frequency synchronization is perfect. In such a case, the expressions in equations should be viewed as representing the best achievable performance in the presence of log-normal fading.

For rectangular M-ary QAM modulation with coherence detection, the BER calculation in AWGN channel is expressed as

$$P_b(\gamma) = \frac{4(\sqrt{M}-1)}{\sqrt{M}log_2M} Q(\sqrt{\frac{3\bar{\gamma}_b log_2 M}{M-1}}), \quad (23)$$

where $Q(x) = \frac{1}{\sqrt{2\pi}}\int_x^\infty e^{-t^2/2}dt,\ x \leq 0$.

By replacing the (23) into (22), the BER performance for different M-QAM modulations in CM1 and for QPSK in different UWB channel models is shown in Figure 3 and Figure 4, respectively. For comparison purposes, the BER curves in AWGN channel and Rayleigh fading channel are also provided. It is observed from the figures that the BER performance for QPSK in UWB fading channel is better than that in Rayleigh fading channels. Furthermore, the BER performance is better in the UWB channel models with less severe multipath fading [5][28].

V. Spectral Efficiency Analysis

On the basis of the analysis of the BER performance in MB-OFDM UWB systems, the spectral efficiency with equal power allocation and equal bit allocation is analyzed in this section. The objective of this section is to demonstrate the motivation of proposing a dynamic power and bit allocation algorithm. The performance analyzed in this section will be compared with the performance of the proposed allocation algorithm in the next section.

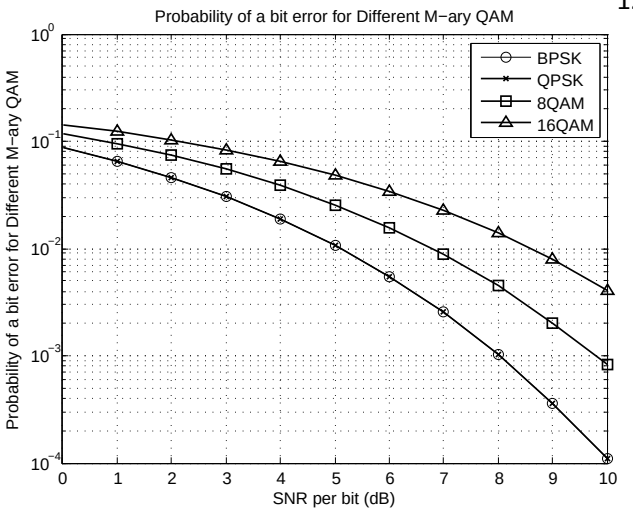

Fig. 3. BER for Different MQAM in CM1

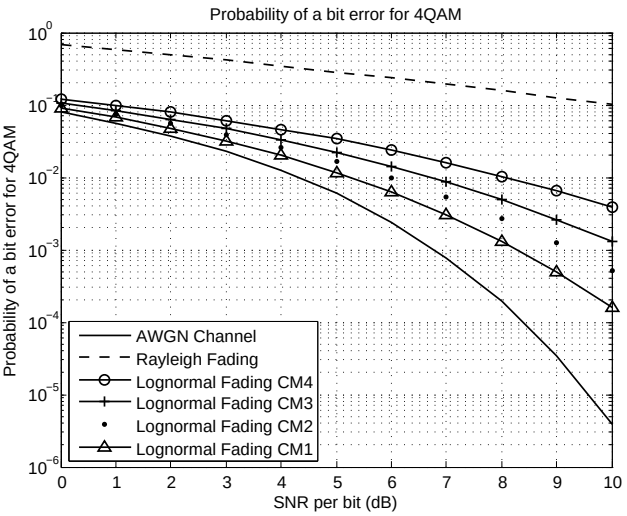

Fig. 4. BER for Different Channel Models

In the MB-OFDM UWB system, the total available transmitted power can be denoted as P_{av}. Since the maximum mean PSD for UWB system is limited to -41.3dBm/MHz, the average maximum allowable transmitted power of the system P_{max} can be approximated as

$$P_{max}\ (dB) = -41.3 \text{ dBm/MHz} + 10log_{10}(f_H - f_L), \quad (24)$$

where f_H and f_L denote the higher and lower frequency of the operating bandwidth in MHz [5]. When the total available transmitted power is $P_{av} = P_{max}$, it is intuitively clear that to maximize the total number of bits which can be allocated into a subband under the power and BER constraints, the optimal strategy should be to equally allocate the transmitted power $P_t(i) = \tilde{P}_{max} = P_{av}/N$ to each subcarrier [27]. The spectral efficiency performance with equal power allocation is analyzed when the available power $P_{av} < P_{max}$.

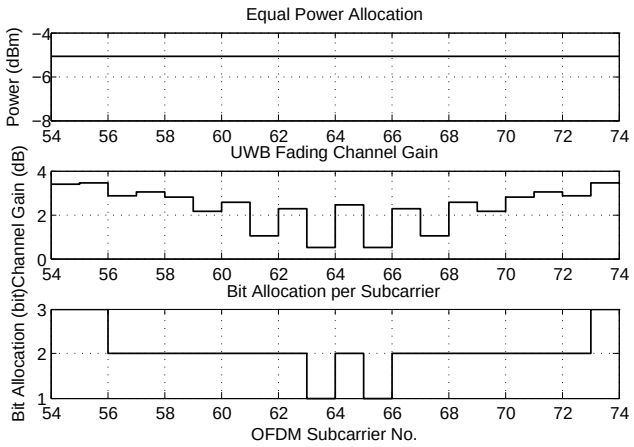

Fig. 5. Bit Allocation in CM1

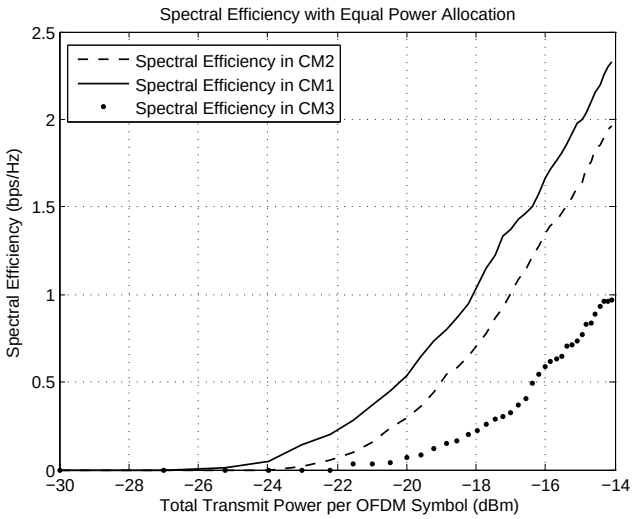

Fig. 6. Spectral Efficiency in CM1

The data bits are dynamically allocated in the OFDM UWB transmitter when the total transmitted power is equally allocated, as illustrated in Figure 5. In this figure, it is observed that there are more bits being allocated to the subcarriers with higher channel gain (less channel multipath fading). Furthermore, the performance of the spectral efficiency in CM1 to CM3 as a function of the total transmitted power per OFDM symbol is illustrated in Figure 6. It can be seen that the spectral efficiency is increased exponentially as the transmitted power increases. The allocation algorithm discussed in the next section can significantly increase the spectral efficiency under the constraints from the primary users while keep the number of iterations to convergence small.

VI. Dynamic Power and Bit Allocation Scheme

In this section, the proposed dynamic power and bit allocation algorithm is presented. The spectral efficiency maximization algorithm is divided into four sections. These are: spectrum sensing, M-QAM zones generation, primary power and bit allocation and advanced power and bit allocation.

TABLE I
Spectral Efficiency Maximization Algorithm

Step	Operations
Step 1	Sense the operating channel, and access the available subcarriers of which the target $\tilde{P}_f$ and $\tilde{P}_d$ are achieved for M-QAM zones generation in step 2.
Step 2	Generate a series of M-QAM zones in each available subcarrier by determining the minimum required transmitted power $P_k(i)$ of the ith subcarrier for reliable reception of the kth order M-QAM symbol.
Step 3	Equally allocate the total available power P_{av} among all the N subcarriers in a sub-band, and specify the order of the M-QAM to use in each subcarrier by identifying the M-QAM zones $Z_k(i)$ where $P_t(i)$ falls in.
Step 4	Collect the excessively allocated power in step 3, and iteratively allocate the collected power using greedy algorithm to the subcarrier that requires the least additional power for using a higher order M-QAM while $P_t(i) < \tilde{P}_{max}$.

In the proposed algorithm, the steps of spectral efficiency maximization are summarized in Table I and described in detail as follows.

A. Optimization Problem Formulation

The optimization problem is formulated as follows:

$$\arg\max_{P_t(i)} \sum_{i=1}^{N} \mathbf{B}(i),\ \mathbf{B}(i) \subseteq \mathbf{Z}, \tag{25}$$

subject to

$$p_e \leq \tilde{p_e} \tag{26}$$

$$0 \leq P_{av} \leq P_{max} \tag{27}$$

$$0 \leq P_t(i) \leq \tilde{P}_{max} \tag{28}$$

$$\tilde{P_d} \leq P_d \leq 1,\ 0 \leq P_f \leq \tilde{P_f}, \tag{29}$$

where in (25), the parameter $P_t(i)$ is the power allocated to the ith subcarrier for data transmission, N is the total number of the UWB subcarriers, and $\mathbf{B}(i)$ is an integer number of the loaded information bits in the ith subcarrier under conditions. In (26), p_e is the BER of the system, and $\tilde{p_e}$ is the required BER of the MB-OFDM UWB system.

It is observed from (25) to (29) that the spectral efficiency maximization problem in MB-OFDM UWB systems is a non-convex optimization problem which is NP-hard [29], since the variable $\mathbf{B}(i)$ in the objective function (25) is limited to some integer value. To effectively solve this optimization problem, the heuristic greedy algorithm [11] is adopted in this paper.

B. Spectrum Sensing

The spectrum sensing procedure determines the probability that a subcarrier is utilized by the cognitive UWB system. The procedure also determines the fraction of time for UWB data transmission α_i in the ith subcarrier. Thus, the number of the loaded information bits in the ith subcarrier under conditions $\mathbf{B}(i)$ in (25) can be expressed as

$$\mathbf{B}(i) = B(i)\alpha_i(1 - P_f)(1 - P(H_{1_i})), \tag{30}$$

where $B(i)$ is the bits loaded in the ith subcarrier, and $P(H_{1_i})$ is the probability that the primary user is transmitting

or receiving within the spectrum of the ith subcarrier. It is assumed that the value of $P(H_{1_i})$ follow a Poisson process with intensity set to $\lambda = 1$, which represents the average number of transmissions per 1ms from the primary users. Hence, $P(H_{1_i}) = p(1; \lambda T_{txop_i})$, where $p(x; \lambda t) = \frac{e^{-\lambda t}(\lambda t)^x}{x!}$. For simplicity, the parameter P_f in (30) is approximated by $P_f = \bar{P}_f$.

C. M-ary QAM Zones Generation

The M-QAM modulation constellation size $M_k(i)$ is restricted to $M_k(i) = 2^k$, $(k = 1, 2, 3, ..., K)$. The rectangular QAM is assumed when $k > 1$ due to energy efficiency and ease of implementation [21]. It is considered that the cognitive UWB users can gather the instantaneous channel state information (CSI) of all links [27]. Thus, the minimum required transmitted power $P_k(i)$ in the ith subcarrier for reliable reception of the kth order M-QAM symbol can be determined as discussed in Section IV.

Then, a series of M-QAM zones $Z_k(i)$, $(k = 0, 1, 2, 3, ..., K)$ are generated by assigning

$$Z_k(i) = [P_k(i), P_{k+1}(i)) \qquad k > 0 \qquad (31)$$

$$Z_0(i) = [P_0(i), P_1(i)) \qquad k = 0, \qquad (32)$$

where $[\cdot)$ represents a half-open interval, and $P_0(i) = 0$ means that no transmission power is required. The kth order M-QAM will be used in the ith subcarrier when the allocated power $P_t(i) \in Z_k(i)$. Figure 7 shows the M-QAM zone generation. Five M-QAM zones are generated for each subcarrier. For example, the required transmitted power $P_k(3)(k = \{1, 2, 3, 4\})$ in the subcarrier-3 is lower than $P_k(2)$ in the subcarrier-2 for each kth order M-QAM due to the higher channel gain of the subcarrier-3.

D. Primary Power and Bit Allocation

In the step 3 of the algorithm, the transmitter initially splits P_{av} equally among all the N subcarriers in a sub-band as $P_t(i) = \bar{P}_t(i) = P_{av}/N$. Therefore, the constellation size $B(i)$ allocated to the ith subcarrier can be determined as

$$B(i) = log_2(M_k)\alpha(i), \qquad (33)$$

where $\alpha(i) = \{0, 1\}$ is the allocation coefficient, and is expressed as

$$\alpha(i) = \begin{cases} 1 & P_t(i) \in Z_k(i) \\ 0 & P_t(i) \in Z_0(i). \end{cases} \qquad (34)$$

An example is shown in Figure 7, where zero bit is assigned to subcarrier-1 since $\bar{P}_t(i)$ falls into the zone-0 of subcarrier-1, while 2 bits are assigned to subcarrier-2 for 4-QAM since $\bar{P}_t(i)$ falls into the zone-2 of subcarrier-2.

E. Advanced Power and Bit Allocation

It is noticeable in Figure 7 that $\bar{P}_t(i)$ of each subcarrier exceeds the required transmitted power $P_k(i)$. Hence, at the beginning of step 4, the transmitter decreases the allocated power $P_t(i) = \bar{P}_t(i)$ to $P_t(i) = P_k(i)\alpha(i)$. The excessive

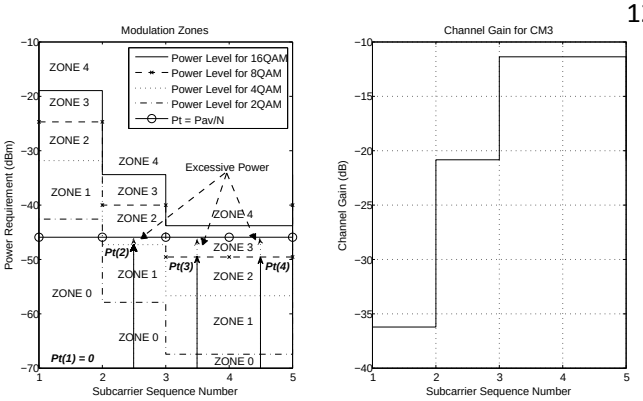

Fig. 7. M-ary QAM zone generation over CM3

allocated power P_m is collected for the advanced allocation, and is given by

$$P_m = P_{av} - \sum_{i=0}^{N-1} P_t(i). \qquad (35)$$

Then, P_m is optimally distributed to the subcarriers by using the greedy algorithm to maximize the number of bits to be carried by each subcarrier [11]. Therefore, the additional power $\Delta\mathbf{P_t} = \{\Delta P_t(i), (i \in [0, N-1])\}$ needed to promote the order of the M-QAM in each subcarrier is determined by

$$\Delta P_t(i) = P_{k+1}(i) - P_k(i). \qquad (36)$$

Next, the ith subcarrier with the minimum $\Delta P_t(i) = min(\Delta\mathbf{P_t})$ is chosen to be promoted to use a higher order M-QAM by assigning more power and bits to this subcarrier when $\Delta P_t(i) \leq P_m$. Thus, $P_t(i)$ and $B(i)$ allocated to the ith subcarrier are increased to

$$P_t(i) = P_t(i) + \Delta P_t(i) \qquad (37)$$

$$B(i) = B(i) + \Delta B(i), \qquad (38)$$

where $\Delta B(i) = log_2(M_{k+1}) - log_2(M_k)\alpha(i)$.

After each iteration, P_m is decreased to

$$P_m = P_m - \sum_{j}^{J} min(\Delta\mathbf{P_t}(j)),\ 0 \leq j \leq J \leq N-1, \qquad (39)$$

where j denotes the jth iteration, and J stands for the advanced power and bit allocation. The process will be terminated when $P_m < \Delta P_t(i) = min(\Delta\mathbf{P_t})$.

Finally, the expression $\sum_{i=1}^{N} \mathbf{B}(i)$ is maximized by implementing the advanced allocation. The order-of-growth of the proposed algorithm is $(\sum_{i=1}^{N} \mathbf{B}(i) - K)NlogN$, where K is the total number of bit allocated in the primary power and bit allocation process. In the low-SNR regime such as UWB systems, the primary power and bit allocation can significantly lower the total number of algorithm iterations [30].

VII. Simulation Results

In the simulation, a scenario of a point-to-point communication between two cognitive UWB systems is investigated in Matlab. It is assumed that the average number of transmissions per $1ms$ from the primary users within the communication ranges of the UWB systems follow a Poisson process. In the analysis, the spectral efficiency is used as a performance indicator of the spectral efficiency optimization algorithm. It is derived from normalizing the data rate $\sum_{i=1}^{N} \mathbf{B}(i)/T_s$ respect to the operating bandwidth W.

First, an implementation of the primary and advanced allocation schemes is examined over CM3. Subsequently, the spectral efficiency comparison between the primary and advanced allocation is made under different SNR conditions. Then, the optimized spectral efficiency versus target BER $\tilde{p_e}$ over different channel models is analyzed. Finally, the optimized spectral efficiency versus the number of the M-QAM zones is discussed. The parameters of the UWB channel model are listed in [5], and the other parameters used to obtain the simulation results are summarized in Table II.

Furthermore, an application with $T_{txop} = 512$ μs (ACs) is chosen to be activated in the cognitive UWB system. All the results assume a system with a subcarrier spacing of 4.125MHz, N=128 subcarriers, and a Nyquist filter with 0% roll-off and bandwidth 528MHz. The receiver structure employed in this work is based on a coherent detection that assumes perfect channel estimation and no synchronization errors. It is composed of a Discrete Fourier Transform (DFT) demodulator block and parallel to serial converter.

Figure 8 and Figure 9 illustrate the primary and advanced allocation over CM3 with $\tilde{p_e}$ =1e-5, respectively. It is observed in Figure 8 that subcarrier-69 is allocated with zero power and bit in primary allocation due to a low corresponding channel gain of -38 dB. During the advanced allocation, as shown in Figure 9, P_m is iteratively assigned to a subcarrier with the minimum $\Delta P_t(i)$ to allow the subcarrier to use the higher level of M-QAM modulation. For example, subcarrier-74 is promoted from 8-QAM to 16-QAM by increasing the transmitted power from -48 dB to -42 dB. Each subcarrier is allocated with the maximum possible order M-QAM until the available power P_{av} is efficiently employed.

Furthermore, the spectral efficiency comparison between the primary and advanced allocation over CM3 with the number of M-QAM levels set to $M = 4$ is depicted in Figure 10. It is also set $\tilde{p_e} \in$[1e-7, 1e-5] and SNR$_p$ $= \gamma_p$ to -20 dB and -10 dB. The spectral efficiency is significantly improved by at least 25% when the advanced allocation is applied under both SNR$_p$ conditions. Also, it is observed that the optimized spectral efficiency is improved when the value of SNR$_p$ is higher. This result is analyzed in Figure 11 in more detail.

It is illustrated in Figure 11 that the values of the optimized spectral efficiency increase exponentially as the estimated SNR$_p$ value is higher. It is observed that the improvement in spectral efficiency is significant when the SNR$_p$ increases from -20 to -10 dB over CM3, and is minor when the value of SNR$_p$ increases further. This is due to the fact that the required sensing period τ_s decreases exponentially when SNR$_p$ increase, as expressed in (13).

The choice of the number of M-QAM levels depends on how fast the channel is changing as well as on the hardware

TABLE II
Simulation Parameters

Parameter	Value
P_{av}	<-14.1 dBm
$\tilde{P_f}$	0.1
P_{max}	-35.1 dBm
$\tilde{P_d}$	0.9
f_s	528 MHz
γ_p	[-20, -18, ..., 0] dB
Subcarrier No.	128
$\tilde{p_e}$	1e-5$\sim$1e-7
W	4.125 MHz
M-QAM	[2,3,4,8,16]
T_{txop_i}	512 μs
λ	1/ms

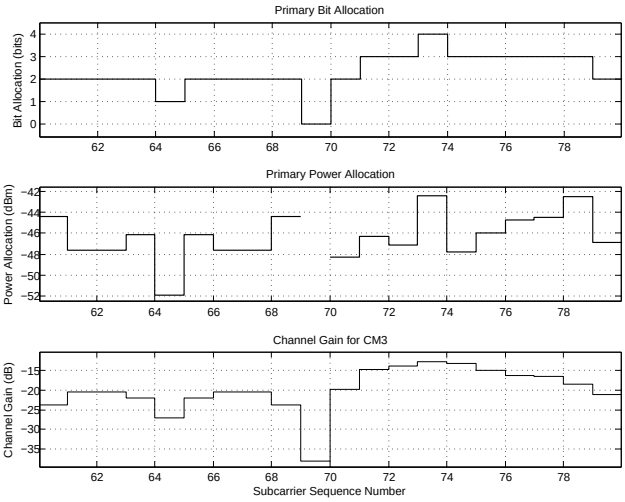

Fig. 8. Primary power and bit allocation

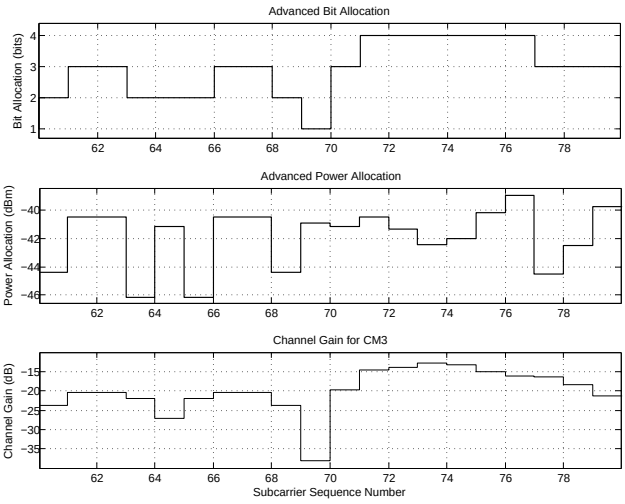

Fig. 9. Advanced power and bit allocation

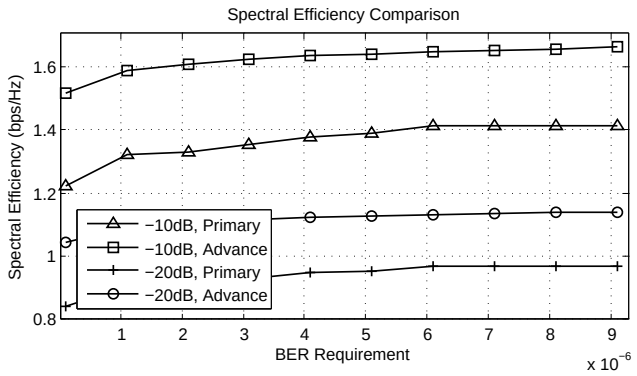

Fig. 10. Primary allocation compared with Advanced allocation, four-point QAM in CM3

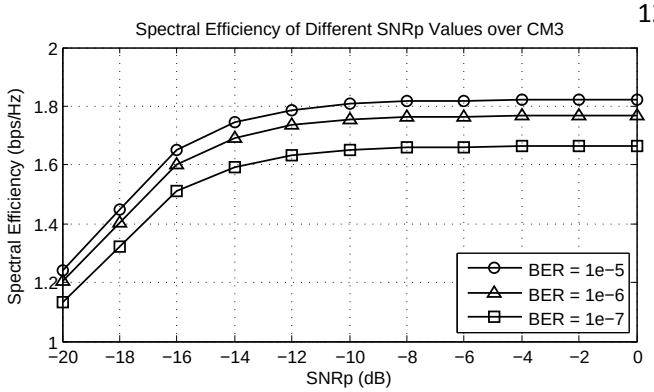

Fig. 11. Optimal Spectral efficiency over CM3 with four-point QAM

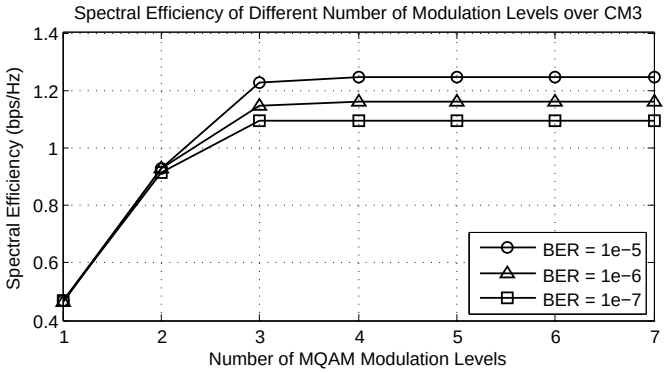

Fig. 12. Optimal Spectral efficiency of different number of modulation levels over CM3, $\text{SNR}_p = -20$ dB

constraints [31]. It is shown in Figure 12 that the improvement in spectral efficiency is significant when the number of M-QAM zones increases from 1 to 4 over CM3, and is minor when the number of M-QAM zones increases further. This is due to the fact that the required transmitted power $P_k(i)$ for a high order M-QAM generally exceeds the maximum allowable transmitted power $\tilde{P}_{max}$ in a subcarrier under the BER requirement $\tilde{p_e}$. Thus, to use a large number of M-QAM levels is necessary only when $max(P_k(i)) < \tilde{P}_{max}$.

VIII. Conclusion and Future Work

This paper presents a novel dynamic power and bit allocation scheme for spectral efficiency maximization in the cognitive MB-OFDM UWB radio system. A new BER expression is derived for an in-depth spectral efficiency analysis of UWB multipath channel. The derivation is based on approximating a sum of independent log-normal random variables as another log-normal random variable using the Fenton-Wilkinson method. Then, the performance of the spectral efficiency of the UWB system with equal power allocation is analyzed. This analysis demonstrates the motivation of the design of the dynamic allocation algorithm. To optimize the spectral efficiency and facilitate the convergence of the dynamic allocation algorithm within a small number of iterations, the optimization algorithm is divided into four sections. The results show that the spectral efficiency of the UWB systems is significantly improved when the advanced allocation is applied. The value of the optimized spectral efficiency is significantly improved with the increase of the received SNR_p value and the number of the M-QAM zones. However, this improvement becomes minor when the SNR_p value and the number of the M-QAM zones are large.

The uncoded BER expression derived in this work provides a foundation for further study of the coded BER expression with primary user and multiuser interference. More comprehensive analysis of the MB-OFDM UWB time and frequency diversity can be conducted in time variant channel model. Then, a new cognitive power and bit allocation algorithm can be further explored and implemented.

Acknowledgment

The authors wish to thank Michael Barry for his insight and inspiration for the work.

Liaoyuan Zeng's work on this paper is funded through Irish Research Council for Science, Engineering & Technology (IRCSET) Scholarship.

References

[1] L. Zeng, S. McGrath, and E. Cano, "Rate maximization for Multiband OFDM Ultra Wideband systems using adaptive power and bit loading algorithm," *Proceedings of the 5th International Conference on Advanced Telecommunications and Systems*, pp. 369–374, May 2009.

[2] I. J. Mitola and G. Q. Maguire, "Cognitive radio: making software radios more personal," *IEEE Magzine on Personal Communications*, vol. 6, no. 4, pp. 13–18, Aug. 1999.

[3] D. Zhang, Z. Tian, and G. Wei, "Spatial capacity of narrowband vs. Ultra-Wideband cognitive radio systems," *IEEE Transactions on Wireless Communications*, vol. 7, no. 11, pp. 4670–4680, Nov. 2008.

[4] G. Bansal, M. J. Hossain, and V. K. Bhargava, "Optimal and suboptimal power allocation schemes for OFDM-based cognitive radio systems," *IEEE Transactions on Wireless Communications*, vol. 7, no. 11, pp. 4710–4718, Nov. 2008.

[5] A. Batra, J. Balakrishnan, G. Aiello, J. Foerster, and A. Dabak, "Design of a Multiband OFDM system for realistic UWB channel environments," *IEEE Transactions on Microwave Theory Techconology*, vol. 52, no. 9, pp. 2123–2138, September 2004.

[6] N. Beaulieu, A. Abu-Dayya, and P. Mclane, "Estimating the distribution of a sum of independent lognormal random variable," *IEEE Transactions on Communications*, vol. 43, pp. 2869–2873, December 1995.

[7] Z. Wang and G. Giannakis, "Wireless multicarrier communications where Fourier meets Shannon," *IEEE Signal Processing Magzine*, vol. 17, no. 3, pp. 29–48, May 2000.
[8] A. Skelton and S. Fu, "An improved conditional maximum-likelihood detector for noncoherent UWB communication," *IEEE Communications Letters*, vol. 13, no. 1, pp. 7–9, Jan. 2009.
[9] E. Hossain and V. Bhargava, *Cognitive Wireless Communication Networks*. New York, USA: Springer Science+Business Media, LLC, 2007.
[10] B. T. Ahmed and M. C. Ramon, "On the impact of Ultra-Wideband (UWB) on macrocell downlink of umts and CDMA-450 systems," *IEEE Transactions on Electromagnetic Compatibility*, vol. 50, no. 2, pp. 406–412, May 2008.
[11] T. Cormen, C. Leiserson, R. Rivest, and C. Stein, *Introduction to Algorithms*, 2nd ed. Boston, USA: The MIT Press, 2001.
[12] Y. Chen, G. Yu, Z. Zhang, H. H. Chen, and P. Qiu, "On cognitive radio networks with opportunistic power control strategies in fading channels," *IEEE Transactions on Wireless Communications*, vol. 7, no. 7, pp. 2752–2760, 2008.
[13] W. Siriwongpairat, W. Su, and K. Liu, "Performance characterization of Multiband UWB communication systems using poisson cluster arriving fading paths," *IEEE Journal on Selected Areas in Communications*, vol. 24, no. 4, pp. 745–751, April 2006.
[14] H. Lai, W. Siriwongpairat, and K. Liu, "Performance analysis of Multiband OFDM UWB systems with imperfect synchronization and intersymbol interference," *IEEE Journal of Selected Topics in Signal Processing*, vol. 1, no. 3, pp. 521–534, October 2007.
[15] C. Snow, L. Lampe, and R. Schober, "Performance analysis of Multiband OFDM for UWB communication," *Proceedings of IEEE International Conference on Communications*, pp. 127–130, October 2008.
[16] "UWB channel modeling contribution from intel," IEEE P802.15-02/279-SG3a., Tech. Rep., 2002.
[17] S. Ghassemzadeh, R. Jana, C. Rice, W. Turin, and V. Tarokh, "Measurement and modeling of an Ultra-Wide Bandwidth indoor channel," *IEEE Transactions on Communications*, vol. 52, no. 10, pp. 1786–1796, October 2004.
[18] D. Cassioli, M. Win, and A. Molisch, "The Ultra-Wide Bandwidth indoor channel: From statistical model to simulations," *IEEE Journal on Selected Areas in Communications*, vol. 20, no. 6, pp. 1247–1257, August 2002.
[19] A. Molisch, "Ultrawideband propagation channels-theory, measurement, and modeling," *IEEE Transactions on Vehicular Technology*, vol. 54, no. 5, pp. 1528–1545, September 2005.
[20] F. Zheng and T. Kaiser, "On the evaluation of channel capacity of UWB indoor wireless systems," *IEEE Transactions on Signal Processing*, vol. 56, no. 12, pp. 6106–6113, Nov. 2008.
[21] J. G. Proakis, *Digital Communications*, 4th ed. New York, USA: McGraw-Hill, 2001.
[22] H. L. V. Trees, *Detection, Estimation, and Modulation Theory*. New York, USA: John Wiley and Sons, 1968.
[23] Y. Zeng and Y. C. Liang, "Spectrum sensing algorithms for cognitive radio based on statistical covariances," *IEEE Transactions on Vehicular Technology*, vol. 58, no. 4, pp. 1804–1815, May 2009.
[24] "High rate Ultra Wideband phy and mac standard," ECMA International, Geneva, Tech. Rep., 2005.
[25] G. L. Stuber, *Principles of Mobile Communication*, 2nd ed. New York, USA: Kluwer Academic Publishers, 2002.
[26] W. H. Tranter, S. K. Sam, T. S. Rappaport, and K. L. Kosbar, *Principles of Communication Systems Simulation with Wireless Applications*. United States of America: Prentice Hall, 2004.
[27] A. Goldsmith, *Wireless Communications*. New York, USA: Cambridge University Press, 2005.
[28] J. Montojo and L. Milstein, "Effects of imperfections on the performance of OFDM systems," *IEEE Transactions on Communications*, vol. 57, no. 7, pp. 2060–2070, July 2009.
[29] S. Boyd and L. Vandenberghe, *Convex Optimization*. Cambridge, United Kingdom: Cambridge University Press, 2004.
[30] G. D. J. Forney and G. Ungerboeck, "Modulation and coding for linear Gaussian channels," *IEEE Transactions on Information Theory*, vol. 44, no. 6, pp. 2384–2415, October 1998.
[31] A. J. Goldsmith and S. G. Chua, "Variable-rate variable-power MQAM for fading channels," *IEEE Transactions on Communications*, vol. 45, no. 10, pp. 1218–1230, Oct. 1997.